Growth of copper, nickel, and palladium films on graphite and amorphous carbon

William F. Egelhoff, Jr. and Gary G. Tibbetts
Physics Department, General Motors Research Laboratories, Warren, Michigan 48090
(Received 4 October 1978)

The growth of films of Pd, Ni, and Cu on amorphous carbon has been studied under ultrahigh vacuum from the lowest coverages detectable to films many atomic layers thick. Since surface diffusion of these metals does not occur on amorphous carbon at room temperature, these metals are present as isolated adatoms at the lowest coverages ($\sim 1/10$ monolayer). The electronic states of the metal adatoms are found by photoemission and Auger spectroscopies to be markedly different from those of the bulk metal. All states have a larger binding energy and the valence band is narrower than in the bulk. At increasing coverages (1/4–3/4 monolayer) additional metal atoms fill the gaps between adatoms, and a discontinuous film develops. As a result the electronic states become more like those in the bulk. As coverages increase into the range of several atomic layers, the films are almost continuous, and the electronic states are those of the bulk metal. In contrast to this, ultraviolet photoelectron spectra show that even at the threshold of detectability, Pd, Ni, and Cu atoms deposited on the basal plane of cleaved graphite nucleate into clusters sufficiently large to exhibit valence-band and core-binding energies characteristic of bulk metals.

INTRODUCTION

The rapid expansion in the past two decades of the fields of thin-film physics and epitaxial growth has stimulated a widespread interest in the fundamental physical principles governing the microscopic phenomena which occur during the initiation of the thin-film deposition and epitaxial growth.[1] However, technical difficulties in the investigation of these microscopic phenomena have limited progress in fundamental understanding. Meanwhile, rapid development has occurred in an empirical methodology describing important macroscopic principles. The occurrence of such uneven progress in these technologically important fields makes investigation of the microscopic principles a very fertile area for recently developed techniques of surface physics such as ultraviolet photoelectron spectroscopy (UPS).

The development of UPS as a surface physics technique has occurred within the past five years in response to the importance of understanding the electronic structure of surfaces.[2] The technique has been very successful in elucidating changes in electronic structure which occur when gaseous molecules and atoms are adsorbed on solid surfaces. With its high sensitivity and good resolution, UPS is ideally suited to study the valence-band properties of very low concentrations of metals deposited on nonmetal supports. These properties are of key importance for understanding the role of small particles in catalysis and epitaxy.

Of even more fundamental interest in such studies is an increased understanding of how bulk electronic structure evolves during growth of metal clusters. A thorough comprehension of the transition from isolated atoms to bulk material is of key importance in solid-state physics.

The ideal model systems selected for this work were Pd, Ni, and Cu on graphite. These three metals were selected for the ease with which they can be vapor deposited as well as for their technological importance. Graphite was chosen as an ideal nonmetallic substrate because its electrical conductivity avoids problems of sample charging during photoemission experiments. In spite of this conductivity, graphite is nonmetallic in all of its chemical and physical properties. Graphite and its surface properties are also of intrinsic interest because of its many important technological functions.

EXPERIMENTAL

These experiments were performed in a baked ultrahigh-vacuum system with a base pressure of 3×10^{-8} Pa (2×10^{-10} Torr). Samples of stress annealed pyrolitic graphite (Union Carbide) were cleaved with the standard Scotch tape peel procedure to expose only the basal (0001) plane and immediately installed in the vacuum system. After achieving pressure in the 10^{-8} Pa range the graphite could be completely cleaned of impurities by heating to 800 °C. The surface was composed of crystallites exposing only the (0001) planes and gave a sharp low-energy-electron diffraction (LEED) pattern. This surface will be referred to as the crystalline surface. The other surface used in these studies was the amorphous carbon surface. It was produced from the crystalline surface by extensive ion bombardment (10 μA/cm^2) with 2 Kv Ar^+ ions followed by annealing at 800 °C to remove imbedded Ar. This caused the LEED beams to be replaced by an isotropic background.

 © 1979 The American Physical Society

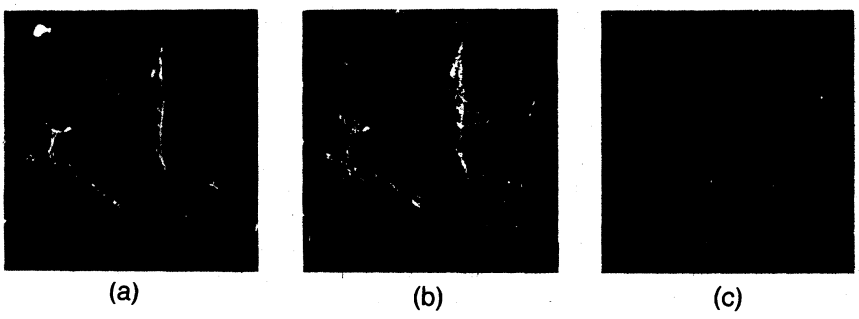

FIG. 1. (a) Negative sample-current-scanning electron micrograph of copper deposited on crystalline graphite. (b) Cu x-ray emission micrograph taken from the same area. (c) X-ray background from the above area.

The absence of any detectable LEED beams (including the specular) established this surface as amorphous carbon.

All metals of this study were deposited by evaporating high-purity foils wrapped around a tungsten filament. These metals were deposited simultaneously on the substrate and on a quartz-crystal thin-film monitor whose calibration was found to be in good agreement with our own estimates of film thickness based on x-ray photoemission peak areas.

We have previously discussed the rest of the apparatus in detail.[3] All photoemission data presented here are angularly integrated over all polar angles from 20° to 60°.

GROWTH MORPHOLOGY

Two fundamentally different substrate surfaces have been employed in this study of cluster growth, the basal plane of graphite and the amorphous carbon surface produced by ion bombarding the basal plane. The basal plane of graphite is a hexagonally symmetric layer of carbon atoms. Bonding in

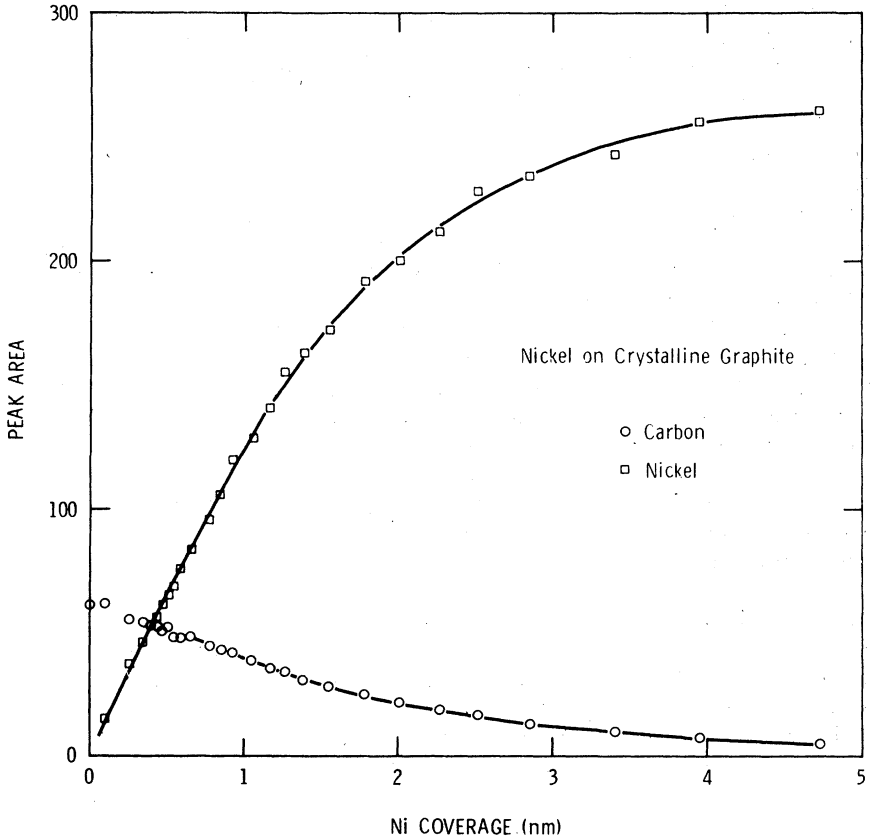

FIG. 2. X-ray photoemission peak areas of the carbon 1s and nickel $2p_{3/2}$ peaks as a function of Ni overlayer thickness on crystalline graphite.

the plane is extremely strong, yet the layers adhere to one another only by weak Van der Waals bonding. This suggests that vapor-deposited metal atoms should be at most weakly bonded to the basal plane of graphite. This suggestion is supported by the studies on the absorption-desorption kinetics of Cu and Au on the basal plane of graphite by Arthur and Cho.[4] They found that vapor-deposited metal atoms behave as a two-dimensional gas on the basal plane, diffusing until they encounter a surface defect to which they can bond strongly and form a nucleation center. Subsequent metal atoms bond to these nucleation centers so that clusters grow radially outward. Our direct observation confirms this growth mechanism. A good example is presented in Fig. 1 for a Cu coverage of 5×10^{14} atoms/cm^2 ($\sim\frac{1}{4}$ monolayer) on the basal plane of graphite. The Cu x-ray image of the surface shows the same features as the negative sample current image of the same region demonstrating that the Cu atoms nucleate at surface defects. The growth of vapor-deposited metals on the basal plane of graphite represents one extreme in the mechanism of nucleation and growth.

The other extreme is found for the amorphous carbon surface produced by ion bombardment of the basal plane. This surface is effectively saturated with defects so that the vapor-deposited metal atoms absorb at the site of impact. Consequently the electron micrographs of the amorphous surface [analogous to those of Fig. 1(a)] showed that the deposited metal atoms are uniformly distributed and at low coverage do not form the macroscopic clusters seen in Fig. 1(a). For higher resolution, transmission electron micrographs have been taken of copper on the amorphous surface. With the 0.05-μm resolution available to us, no clustering could be observed. However, by using more powerful transmission electron microscopes and cluster amplification by Zn atoms, formation of Pd, Ni, Ag, and Au clusters on amorphous carbon has been studied by Hamilton *et al.*[5] They demonstrated by transmission electron microscopy that at coverages less than $\frac{1}{4}$ monolayer the deposited metal atoms are predominantly adsorbed as isolated adatoms and that at higher coverages clusters grow by random adsorption of metal atoms.

Further morphological information is obtained by close study of how the photoemission peak areas vary with overlayer coverage. Figure 2 presents the x-ray photoelectron spectroscopy (XPS) peak intensities for the nickel and carbon core electrons as a function of the amount of nickel deposited on crystalline graphite. As expected the nickel peak intensity increases and the carbon peak

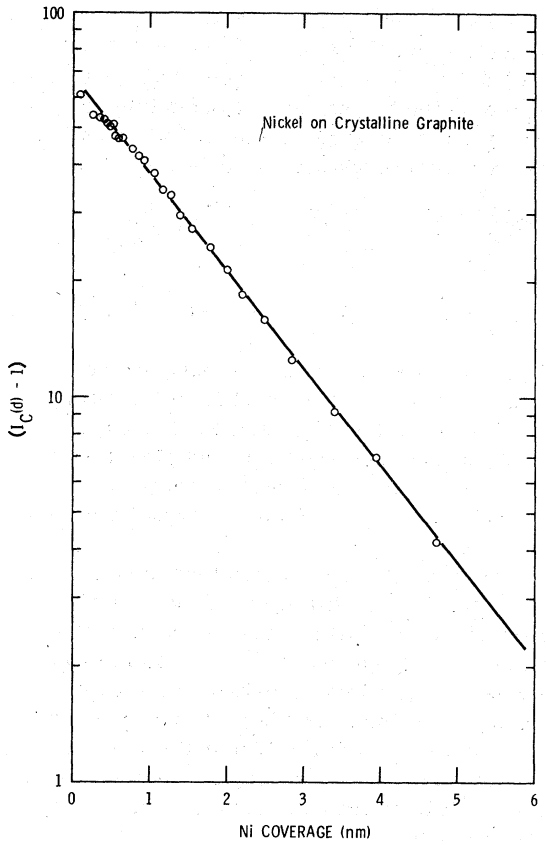

FIG. 3. Carbon 1s photoemission peak area from Fig. 2 as a function of nickel overlayer thickness. The function plotted, carbon area minus 1 area unit, takes account of the small substrate area left bare at high Ni coverages.

intensity decreases with coverage. It may, however, be seen that even after many layers are deposited, the carbon signal does not quite approach zero. This indicates that the Ni overlayer does not completely cover the substrate. The observed XPS peak area of the carbon, $I_c(d)$, will be a function of the Ni layer thickness d and the inelastic scattering mean free path of the carbon 1s (kinetic energy 968 eV) electrons in Ni, λ_c. If A_0 is the constant fraction of the surface area on which Ni does not stick, the remainder of the surface being uniformly covered,

$$I_c(d)=I_c(0)[A_0+(1-A_0)e^{-d/\lambda_c}]$$

or

$$\ln\left(\frac{1}{I_c(0)(1-A_0)}\left\{I_c(d)-I_c(0)A_0\right\}\right)=-\frac{d}{\lambda_c}\,.$$

In Fig. 3 we plot the function in curly brackets, with $I_c(0)A_0=1$ determined from the asymptote of the carbon signal $I_c(\infty)$ of Fig. 2. The experimental points fall on a good straight line and yield λ_c

$=1.7$ nm.

Figure 2 also shows the increase in Ni $2p_{3/2}$ peak as a function of Ni coverage. In the same approximation the Ni peak area $I_N(d)$ will be determined by the mean free path of Ni $2p_{3/2}$ photoelectrons[6] (kinetic energy 396 eV) in Ni, λ_N.

$$I_N(d)=I_N(\infty)[(1-A_0)][1-e^{-d/\lambda_N}]$$

or

$$\ln\left(\frac{1}{I_N(\infty)(1-A_0)}\{(1-A_0)I_N(\infty)-I_N d)\}\right)=\frac{-d}{\lambda_N}.$$

In Fig. 4 we plot the function in curly brackets with the first term determined from the asymptote of the nickel signal of Fig. 2. The experimental points fall on a straight line and yield a value λ_N of 1.4 nm. For the case of Ni above, A_0 is nearly 0; however, for Pd on amorphous carbon, A_0 approaches 0.3.

Data from other experiments tend to confirm the picture that the metallic layers deposit uniformly on part of the crystalline surface leaving other parts completely uncovered. Electron microscopic studies[7] of Cu films deposited on rocksalt at 300 K typically show sizable portions of the substrate uncovered even for 10-nm-thick films. Moreover, our own microscopic observations of Cu on crystalline graphite in Fig. 1 show similar cluster growth.

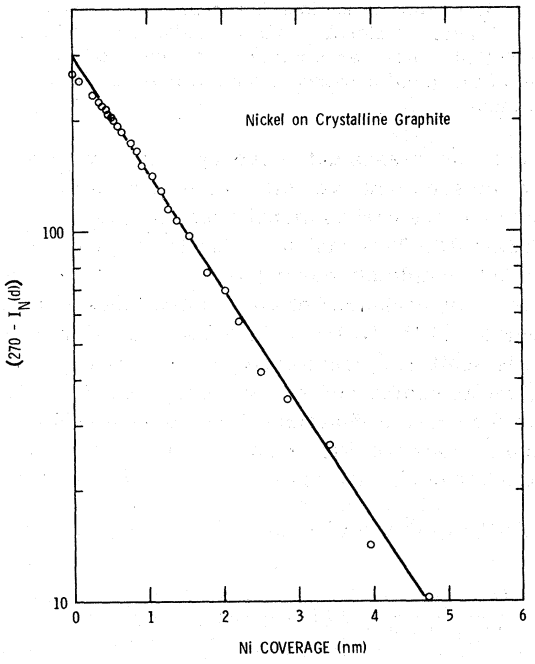

FIG. 4. Nickel $2p_{3/2}$ photoemission peak area from Fig. 3 as a function of nickel overlayer thickness. The function plotted is 270 area units minus nickel peak area.

PHOTOEMISSION RESULTS

Figure 5 presents plots of the Cu $2p_{3/2}$ binding energy, determined by x-ray photoemission, as a function of Cu coverage on amorphous carbon and crystalline graphite. For coverages above 0.3 nm, the $2p_{3/2}$ binding energy is not affected by the substrate morphology. For the lowest coverages, the Cu deposited on crystalline graphite had a slightly higher $2p_{3/2}$ binding energy than bulk Cu. This is consistent with a very small concentration of preferred sites on this largely homogeneous surface. Moreover, it is consistent with the formation of large Cu clusters at even the lowest observable coverages. Similar results have been observed for Cu deposited at 100 K on crystalline graphite, indicating that surface diffusion of Cu on crystalline graphite is rapid even at low temperatures.

Figure 5 also shows that the Cu $2p_{3/2}$ binding energy for Cu deposited on amorphous carbon is 0.6 eV larger than that displayed by bulk copper at very low coverages. Similar shifts were observed for the other copper core levels. These observations are consistent with the presence of numerous single-atom or low-coordination binding sites at low coverage. This pattern is also followed very closely by the Ni $2p_{3/2}$ and the Pd $3d_{3/2}$ and $3d_{5/2}$ binding energies, and clearly the same morphological conclusions apply.

The ultraviolet photoelectron spectra of deposited Cu, Ni, and Pd show some similar features, but are rich in detail. Figure 6 shows HeI (21.2 eV) photoemission spectra for clean graphite before and after the deposition of 0.5 nm of Ni. The difference spectrum illustrates the changes induced by the overlayer. For this spectrum and

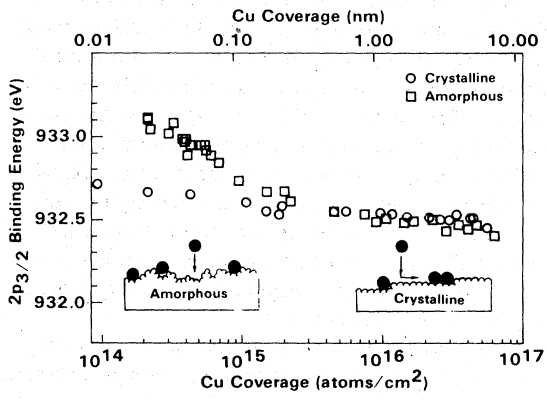

FIG. 5. Copper XPS $2p_{3/2}$ peak position as a function of overlayer thickness on both the crystalline and amorphous substrates. The inserts show how metallic overlayers deposited on crystalline graphite aggregate at defect sites, whereas in thin overlayers deposited on amorphous carbon the metal atoms remain dispersed.

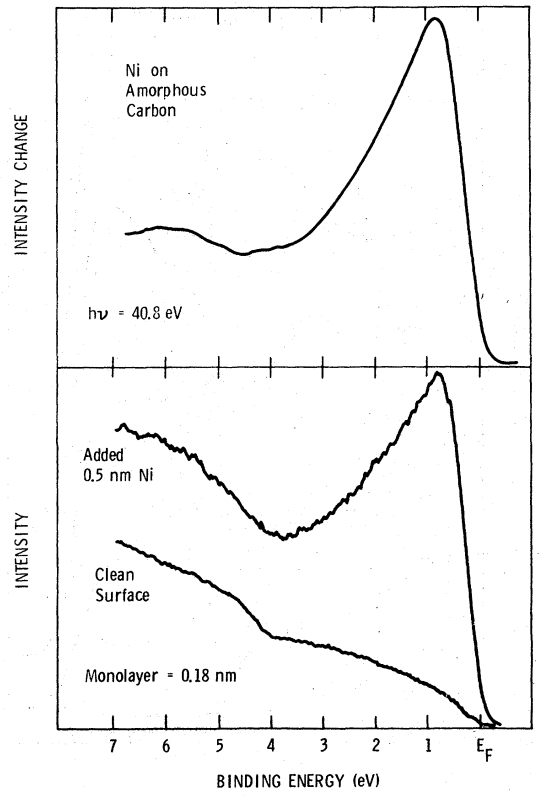

FIG. 6. Bottom panel shows He I ultraviolet photoemission spectra for the amorphous carbon substrate and for the substrate with a Ni overlayer. Top panel shows difference spectrum attributable to the overlayer alone.

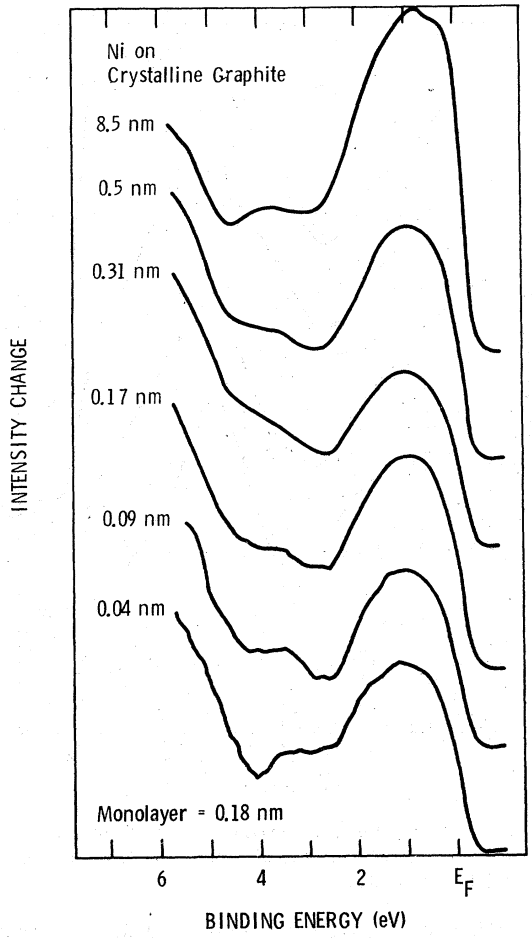

FIG. 7. He I ultraviolet photoemission difference spectra for various thicknesses of nickel deposited on crystalline graphite.

all of those following we have followed the same subtraction procedure. The intensity of the substrate spectrum used in the subtraction is weighted according to the fraction of the substrate photoemission which can escape through the metal overlayer. Our procedure makes use of the known escape depths as a function of photoelectron kinetic energy.[2] Figure 7 shows difference photoemission spectra for different coverages of Ni on crystalline graphite. The coverages of Ni for which each spectrum is made is shown on the graph in nanometers. Note that the midpoint of the upper d-band edge is always found at E_f in these spectra. Also the d-band width in the spectra are the same except for the one made at highest coverage. These spectra are entirely consistent with the above cluster behavior. As the coverage increases from the very lowest values the Ni $3d$-band peak remains at constant position and width because all the Ni at the surface is present as large clusters. The increase in width for the highest coverage spectrum results from the increased d-band interactions in moving from an island to a bulk solid.

He II photoemission spectra, made at 40.8 eV photon energies, confirm these results.

Figure 8 shows similar spectra for Pd deposited on crystalline graphite. The Pd spectrum is broader than the Ni, and is composed of two main peaks. The point of inflection of the low-binding-energy edge of the more weakly bound peak remains at the Fermi energy, for all coverages. This behavior is shown more clearly in the He II spectrum, where the more gently sloping background does not overemphasize the higher-binding-energy portion of the Pd spectrum (Fig. 9).

Figure 10 shows similar UPS data for Cu on crystalline graphite. The upper $3d$-band edge is not affected by coverage changes and the width of the $3d$ band does not increase until more than one monolayer of Cu is deposited.

When these metals are deposited on amorphous carbon (ion-bombarded graphite), the UPS data are quite different. For example, Fig. 11, made

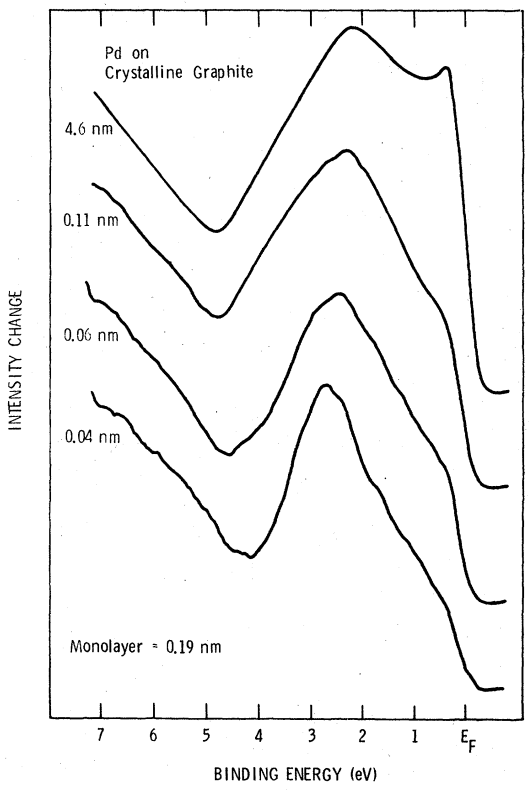

FIG. 8. He I ultraviolet photoemission difference spectra for various thicknesses of palladium deposited on crystalline graphite.

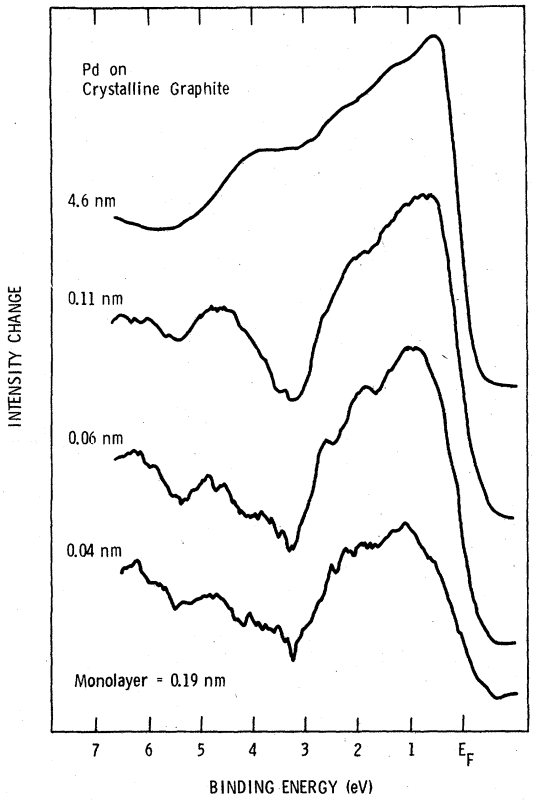

FIG. 9. He II ultraviolet photoemission difference spectra for various thicknesses of palladium deposited on crystalline graphite.

for different Ni coverages shows that at the lowest Ni coverages, the upper 3*d* edge is more strongly bound by 0.5 eV than in the bulk. Likewise, the 3*d* band narrows with decreasing coverage, even compared to spectra made at less than 1 monolayer. These two changes indicate that the lowest coverage UPS is representative of individual Ni atoms bound at defect sites. The 3*d* band is neither as tightly bound nor as narrow as it would be in atomic Ni, indicating some electronic interaction with the graphite and some extra-atomic relaxation around the Ni atoms by graphite valence electrons during photoionization.

The results of Fig. 11 also clarify a point that has been widely discussed in recent literature. The controversy is over the precise interpretation of the peak in the nickel photoemission spectra at a binding energy of 6 eV. The data of Fig. 11 establish that the peak is observed even for isolated nickel adatoms. This means that the peak at 6 eV is not a bulk property of nickel having a band-structure-based interpretation, instead it is an intrinsic property of the nickel atom. The precise origin of the peak is established by noting that Moore's tables of atomic energy levels predicts that the 6 eV peak corresponds in energy to a nickel ion in the d^8p final state, i.e., with a valence electron promoted into the 4*p* atomic orbital. Since the 6 eV peak is observed even for bulk nickel it is properly referred to as a quasiatomic excitation accompanying the photoemission process. We have recently discussed this interpretation in greater detail.[9] The peak at 3.5 eV in the low-coverage spectra in Fig. 11 may be the result of the dip seen in the clean-surface spectrum at that energy in Fig. 6. If the dip is obscured by deposition of nickel then this feature will appear as a peak in the difference spectrum. At larger coverages this will not be manifest because essentially all the photoemission comes from the overlayer. For these reasons we have not interpreted the 3.5-eV peak in terms of initial-state properties.

UPS data for Pd-covered amorphous carbon in Fig. 12 reveal similar tendencies. The Pd upper 4*d* edge becomes more strongly bound at lowest coverages, and the 4*d* band narrows. Figure 13 shows entirely similar effects for Cu deposited on amorphous carbon.

Studies of the work-function change of the graphite surface as a function of concentration of deposited Pd and Cu show that the above spectral

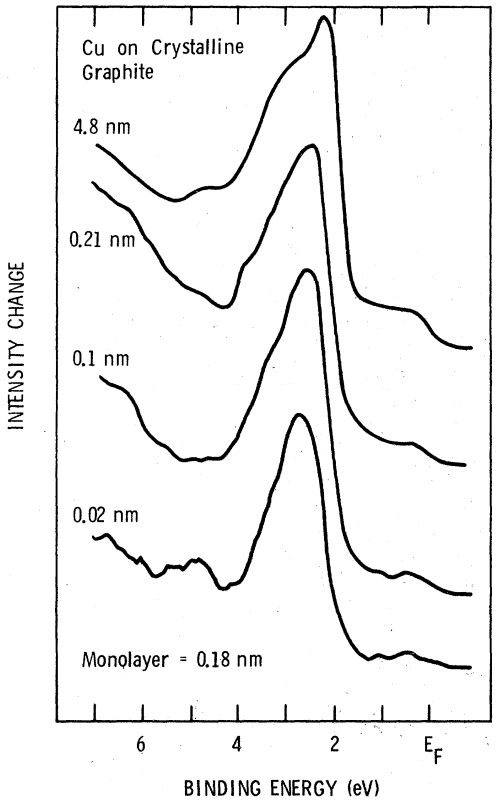

FIG. 10. He I ultraviolet photoemission difference spectra for various thicknesses of copper deposited on crystalline graphite.

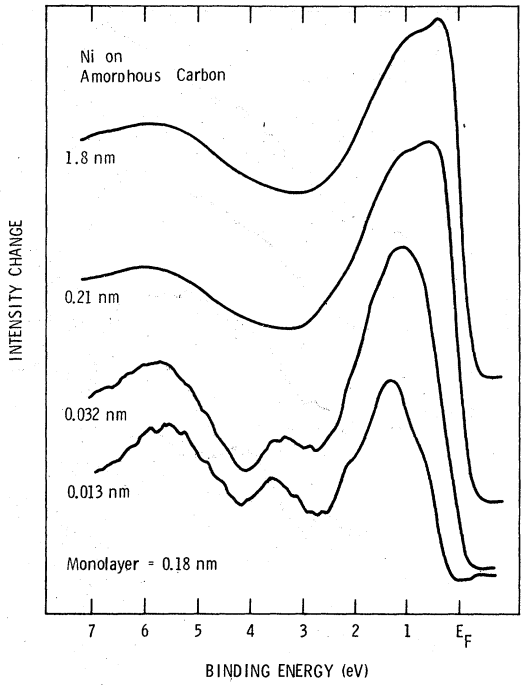

FIG. 11. He I ultraviolet photoemission difference spectra for various thicknesses of nickel deposited on amorphous carbon.

changes are not due to simple electron transfer from the metal overlayer to the substrate at lowest coverages. These measurements show a work-function decrease of 0.2 eV on deposition of a Cu monolayer, whereas the work function increases by 0.2 eV on depositing a Pd monolayer.

The Cu *LMM* Auger spectrum was also studied as a function of Cu coverage on clean and amorphous carbon in order to see any large energy shift which would be representative of the different degrees of electronic relaxation between single atoms and the bulk metal. The shifts in this Auger peak were small and consistent with those observed in the uv spectra.

DISCUSSION

The experimental results obtained here conflict strongly with those obtained by Mason, Gerenser, and Lee[10] for Pd on evaporated carbon substrates. Mason *et al.* observed a 2.3-eV shift in the $3d_{5/2}$ peak position, whereas we observe a 0.6-eV shift between low and high coverage. Likewise they observe a 2.3-eV shift in the upper $4d$-band edge, whereas we observe a 0.5-eV shift between low and high coverage. We attribute the excessive shifts observed by Mason *et al.* to their technique of sample preparation in one vacuum system followed by transfer through air and measurement in another vacuum system. This technique assures that the surfaces are representative of highly oxidized clusters. We were able to obtain very large $2p_{3/2}$ peak shifts at lowest coverages of Ni by exposing our surfaces to air at atmospheric pressure. Our UPS results for Pd on amorphous carbon are generally in agreement with those reported by Unwin and Bradshaw.[11]

In this work we have shown strong qualitative differences between the ultraviolet photoemission spectra of transition metals deposited on the basal plane of graphite and on amorphous carbon. Both the ultraviolet and x-ray photoemission spectra for these metals deposited on the basal plane of graphite have been shown to be characteristic of large cluster growth, even at lowest temperatures and coverages.

The photoemission spectra for these metals deposited on amorphous carbon show considerably larger changes with coverages. At the lowest coverages studied, where we have atoms well dispersed over the surface (Fig. 5), the increase in binding energies over the bulk results partially from the decreased number of nearest neighbor metal atoms. This mechanism is consistent with the smaller increase observed on crystalline

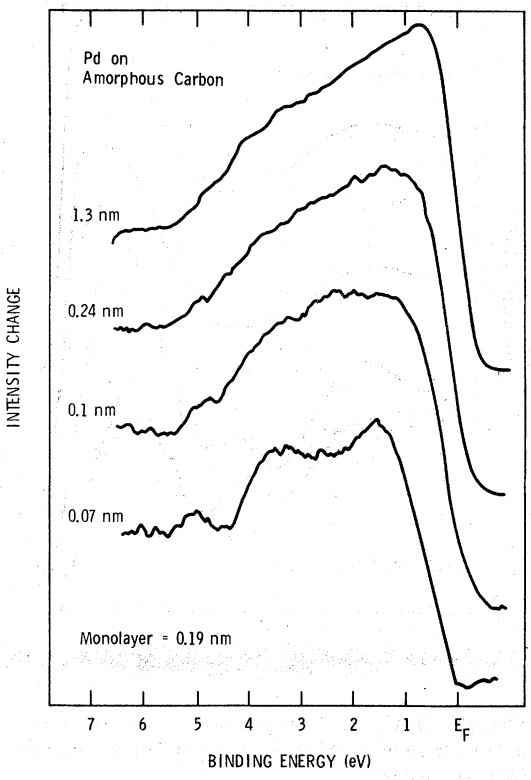

FIG. 12. He II ultraviolet photoemission difference spectra for various thicknesses of palladium deposited on amorphous carbon.

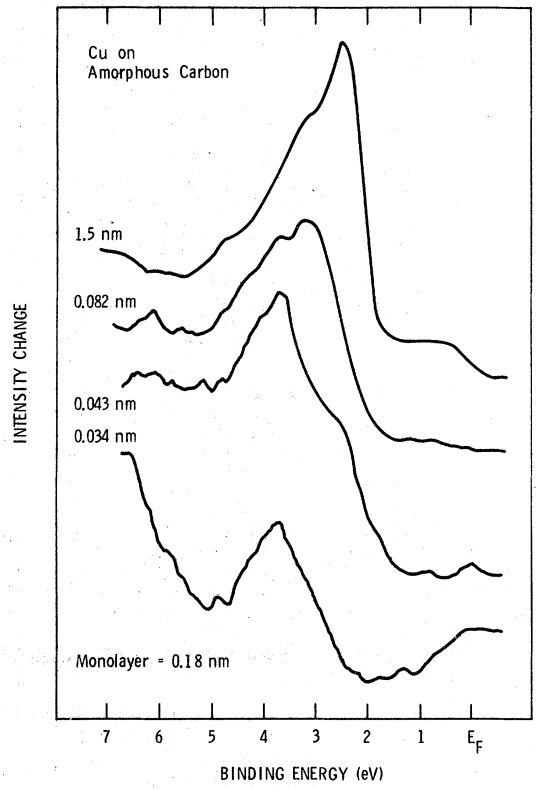

FIG. 13. He I ultraviolet photoemission difference spectra for various thicknesses of copper deposted on amorphous carbon.

graphite, where there is a smaller number of defect sites available on the surface to bind isolated metal atoms.

A mechanism which could cause a decrease in binding energy as particle size increases from isolated atoms through bulk metal, is the increase in extra-atomic relaxation as the number of metallic neighbor atoms increases.

A further mechanism which could cause the decrease in binding energy as the number of adsorbed atoms increases is atomic renormalization of the valence orbitals as metal atoms are packed more closely together. This phenomenon has been discussed extensively in the literature.[12] Our observed binding energy shift cannot be attributed to variations in d-band occupation with coverages because copper, a metal which retains its filled d band in both the atomic and metallic states, exhibits a shift fully comparable with Ni or Pd.

ACKNOWLEDGMENTS

We appreciate the helpful contributions to this work by J. M. Burkstrand, J. C. Tracy, J. R. Smith, J. G. Gay, and the outstanding technical assistance of D. L. Simon.

[1]D. W. Pashley, *Epitaxial Growth*, edited by J. W. Mathews (Academic, New York, 1975).
[2]C. R. Brundle, J. Vac. Sci. Technol. 11, 212 (1974).
[3]G. G. Tibbetts, J. M. Burkstrand, and J. C. Tracy, Phys. Rev. B 15, 3652 (1977).
[4]J. R. Arthur and A. Y. Cho, Surf. Sci. 36, 641 (1973).
[5]J. F. Hamilton, P. C. Logel, and R. C. Baetzold, Thin Solid Films 32, 233 (1976); J. F. Hamilton and P. C. Logel, *ibid.* 23, 89 (1974); J. Catal. 29, 253 (1973).
[6]T. E. Gallon, Surf. Sci. 17, 486 (1978).
[7]J. V. Sanders, *Chemisorption and Reactions on Metal Films*, edited by J. R. Anderson (Academic, New York, 1971), Vol. 1, p. 12.
[8]C. E. Moore, *Atomic Energy Levels as Derived from Analysis of Optical Spectra* (U.S. GPO, Washington, D. C., 1971).
[9]G. G. Tibbetts and W. F. Egelhoff, Jr., Phys. Rev. Lett. 41, 188 (1978).
[10]M. G. Mason, L. G. Gerenser, and S. T. Lee, Phys. Rev. Lett. 39, 288 (1977).
[11]R. Unwin and A. M. Bradshaw, Chem. Phys. Lett. 58, 58 (1978).
[12]C. D. Gelatt, Jr., H. Ehrenreich, and R. E. Watson, Phys. Rev. B 15, 1613 (1977).

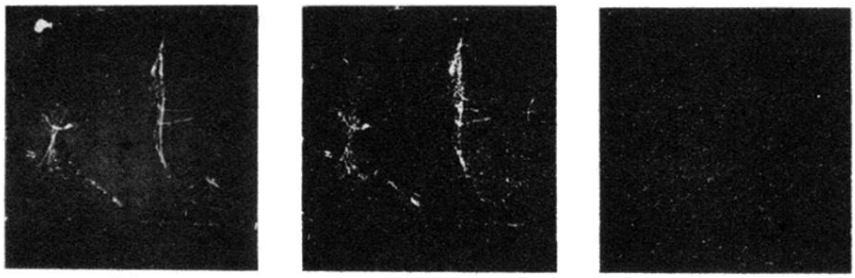

FIG. 1. (a) Negative sample-current-scanning electron micrograph of copper deposited on crystalline graphite. (b) Cu x-ray emission micrograph taken from the same area. (c) X-ray background from the above area.